ESC European Society of Cardiology

Cardiovascular Research (2019) **115**, 154–167
doi:10.1093/cvr/cvy163

Cardiomyocyte-specific deficiency of HSPB1 worsens cardiac dysfunction by activating NFκB-mediated leucocyte recruitment after myocardial infarction

Yana Wang[1†], Jiali Liu[1†], Qiuyue Kong[2], Hao Cheng[2], Fei Tu[1], Peng Yu[1], Ying Liu[1], Xiaojin Zhang[1], Chuanfu Li[3], Yuehua Li[4], Xinxu Min[2], Shuya Du[1], Zhengnian Ding[2], and Li Liu[1,5]*

[1]Department of Geriatrics, Jiangsu Provincial Key Laboratory of Geriatrics, First Affiliated Hospital of Nanjing Medical University, Guangzhou Rd. 300, Nanjing 210029, China; [2]Department of Anesthesiology, First Affiliated Hospital of Nanjing Medical University, Nanjing 210029, China; [3]Department of Surgery, East Tennessee State University, Johnson City, TN 37614, USA; [4]Department of Pathophysiology, Nanjing Medical University, Nanjing 210029, China; and [5]Key Laboratory of Targeted Intervention of Cardiovascular Disease, Collaborative Innovation Center for Cardiovascular Disease Translational Medicine, Nanjing Medical University, China

Received 5 March 2018; revised 6 May 2018; editorial decision 17 June 2018; accepted 28 June 2018; online publish-ahead-of-print 2 July 2018

Time for primary review: 21 days

Aims Inadequate healing after myocardial infarction (MI) leads to heart failure and fatal ventricular rupture, while optimal healing requires timely induction and resolution of inflammation. This study tested the hypothesis that heat shock protein B1 (HSPB1), which limits myocardial inflammation during endotoxemia, modulates wound healing after MI.

Methods and results To test this hypothesis, cardiomyocyte-specific HSPB1 knockout (*Hspb1*$^{-/-}$) mice were generated using the *Cre-LoxP* recombination system. MI was induced by ligation of the left anterior descending coronary artery in *Hspb1*$^{-/-}$ and wild-type (WT) littermates. HSPB1 was up-regulated in cardiomyocytes of WT animals in response to MI, and deficiency of cardiomyocyte HSPB1 increased MI-induced cardiac rupture and mortality within 21 days after MI. Serial echocardiography showed more aggravated remodelling and cardiac dysfunction in *Hspb1*$^{-/-}$ mice than in WT mice at 1, 3, and 7 days after MI. Decreased collagen deposition and angiogenesis, as well as increased MMP2 and MMP9 activity, were also observed in *Hspb1*$^{-/-}$ mice compared with WT controls after MI, using immunofluorescence, polarized light microscopy, and zymographic analyses. Notably, *Hspb1*$^{-/-}$ hearts exhibited enhanced and prolonged leucocyte infiltration, enhanced expression of inflammatory cytokines, and enhanced TLR4/MyD88/NFκB activation compared with WT controls after MI. In-depth molecular analyses in both mice and primary cardiomyocytes demonstrated that cardiomyocyte-specific knockout of HSPB1 increased nuclear factor-κB (NFκB) activation, which promoted the expression of proinflammatory mediators. This led to increased leucocyte recruitment, thereby to excessive inflammation, ultimately resulting in adverse remodelling, cardiac dysfunction, and cardiac rupture following MI.

Conclusion These data suggest that HSPB1 acts as a negative regulator of NFκB-mediated leucocyte recruitment and the subsequent inflammation in cardiomyocytes. Cardiomyocyte HSPB1 is required for wound healing after MI and could be a target for myocardial repair in MI patients.

Keywords Cardiac dysfunction • Cardiac rupture • Myocardial infarction • Inflammation • Heat shock protein B1 (HSPB1)

* Corresponding author. Tel: +86 25 83718836; fax: +86 25 83724440, E-mail: liuli@njmu.edu.cn

† The first two authors contributed equally to this study.

1. Introduction

Due to the limited regenerative capacity of cardiomyocytes, the healing of cardiac tissue after a myocardial infarction (MI) is inadequate compared with healing processes after tissue damage in organs such as the liver. Inadequate healing after MI can lead to heart failure (HF) and ventricular rupture, an extreme and often fatal condition.[1,2] The molecular players modulating wound healing are gradually being identified. However, therapies that ensure optimal healing of injured cardiac tissue have yet to be established, suggesting that a more comprehensive understanding of post-MI wound healing is urgently needed to develop effective targeted therapies.

Wound healing after MI results from a superbly orchestrated series of events, beginning with immune responses to clear the wound of dead cells and matrix debris and followed by activation of the tissue repair programme.[3–5] The early inflammation is a required event for the transition to the later stages of proliferation and tissue repair.[3,4] However, an inflammatory phase that is excessive in magnitude, prolonged, or insufficiently suppressed can lead to sustained myocardial damage and defective healing, thereby promoting infarct expansion, cardiac dysfunction, and lethal cardiac rupture.[3,4,6] Therefore, timely containment and resolution of inflammation is necessary for optimal post-MI repair of cardiac tissue.

Nuclear factor-κB (NFκB) plays a critical role in the post-MI inflammatory response. In infarcted hearts, danger-associated molecular patterns released by dying cardiomyocytes and degraded extracellular matrix (ECM) components are recognized by Toll-like receptors (TLRs) and other pattern recognition receptors on surviving cells, which leads to NFκB activation. Activated NFκB in turn up-regulates the expression of a large panel of proinflammatory mediators including inflammatory cytokines, chemokines, and cell adhesion molecules. Chemokines are inflammatory mediators with an essential role in leucocyte trafficking, and some chemokines such as interferon-γ-inducible protein 10 (IP-10), also exert anti-fibrotic and anti-angiogenic effects.[4,7–9] Thus, inhibiting NFκB inflammatory signalling serves as a promising therapeutic strategy for post-MI wound healing.[10,11]

Heat shock protein B1 (HSPB1), which is also called HSP25 in rodents and HSP27 in primates, encodes a member of the small heat shock protein family. A range of stimuli including oxidative stress, cytokines, and growth factors, can induce HSPB1 expression to acquire tolerance.[12] We and others have demonstrated that HSPB1 attenuates doxorubicin-induced cardiac dysfunction, alleviates cardiac aging, and delays cardiac allograft rejection.[13–15] Recent studies using the Langendorff-perfused heart model demonstrated that non-selective overexpression of HSPB1 improves cardiac contractility within 1 h of reperfusion after 20–35 min of ischaemia.[16,17] However, it is unknown whether HSPB1 specifically within cardiomyocytes can modulate wound healing after MI. Given that HSPB1 in cardiomyocytes attenuated endotoxin-induced cardiac dysfunction and NFκB activation in our previous study,[18] it is possible that HSPB1 in cardiomyocytes plays a role in infarct healing after MI.

To test this hypothesis, we generated cardiomyocyte-specific HSPB1 knockout mice (*Hspb1*$^{-/-}$). HSPB1 expression was up-regulated in wild-type (WT) cardiomyocytes in response to MI, while deficiency of cardiomyocyte HSPB1 impaired infarct healing, as indicated by aggravated remodelling, worse cardiac dysfunction, and increased risk of cardiac rupture. These actions of cardiomyocyte HSPB1 were due, at least in part, to the NFκB-dependent modulation of leucocyte recruitment and the subsequent inflammation. These data suggest that HSPB1 acts as a negative regulator of inflammatory responses in cardiomyocytes and plays an essential role in the healing of injured cardiac tissue after MI.

2. Methods

Additional materials and methods are available in Supplementary material online.

2.1. Generating cardiomyocyte-specific HSPB1 knockout mice (*Hspb1*$^{-/-}$)

HSPB1 conditional knockout mice were generated using *lox*P recombinant system (details shown in Supplementary material online). Knockout of HSPB1 selectively in cardiomyocytes was achieved by cross-breeding HSPB1 conditional knockout mice with αMHC-Cre transgenic mice. Mice were housed in the Model Animal Research Center of Nanjing University and maintained in the Animal Laboratory Resource Facility at Nanjing University. All the experiments were conducted under the guidelines for the Care and Use of Laboratory Animals published by the US National Institutes of Health (NIH Publication, 8th Edition, 2011). The animal care and experimental protocols were approved by the Nanjing University Committee on Animal Care. All the experiments were conformed to the international guidelines on the ethical use of animals.

2.2. Surgical procedures

MI was induced in 8–12-week-old WT and *Hspb1*$^{-/-}$ mice by permanently ligating the left anterior descending coronary (LAD) as described in our previous studies.[19] All the experiments used male mice unless indicated elsewhere. Mice were anaesthetized by sodium pentobarbital (50 mg/kg, intraperitoneal injection). The adequacy of anaesthesia was assayed by the disappearance of righting reflex and pedal withdrawal reflex. After anaesthesia, mice were subjected to mechanical ventilation, chest opening along the left sternal border, and permanent LAD ligation. In sham-operated animals, the same procedure was performed except the LAD occlusion. For analgesia, buprenorphine (0.05 mg/kg) was administrated subcutaneously prior to surgery, and administrated one dose every 8 h for the next 48 h. For tissue collection, mice were sacrificed by overdose anaesthesia (pentobarbital sodium 150 mg/kg intraperitoneal injection) and cervical dislocation. In NFκB inhibition experiments, mice were administrated with pyrrolidinedithiocarbamate (PDTC, 100 mg/kg) intraperitoneally 30 min prior to surgery followed by 100 mg/kg/day for first three days after surgery.[15]

2.3. Mice survival and cardiac rupture

Mice survival was checked twicely per day after surgery. All dead mice received autopsy to dissect the cause of death. The presence of perforation on the infarcted wall, which was accompanied by an intrathoracic blood clot was diagnosed as cardiac rupture.[2]

2.4. Infarct size

Infarct size was determined by triphenyltetrazolium chloride (TTC) staining and expressed as the percentage of infarct over ventricular areas, as previously described.[19]

2.5. Echocardiography

Echocardiography was used to evaluate cardiac function and remodelling at the indicated times post-MI using the Vevo770 system equipped with a 35-MHz transducer (Visualsonics, Toronto, Canada) according to our previous methods.[19] The measurements were performed by an observer blinded to the treatment. Parameters were obtained from M-mode tracings and averaged using three to five cardiac cycles.

2.6. Real-time PCR

Real-time PCR was used to analyse mRNA expression levels according to our previous studies.[20] The expression of genes of interest was expressed as a relative expression compared with that of WT controls. The primers were listed in Supplementary material online, Table S1.

2.7. Western blot

Western blot was performed as described in our previous studies.[19,21] The expression of genes of interest was expressed as a relative expression compared with that of WT controls.

2.8. Statistical analysis

Data are presented as mean ± standard deviation. Comparisons between groups were performed by Student's two-tailed unpaired *t*-test, one-way or two-way analysis of variance analysis followed by Tukey *post hoc* test. Survival curve was analysed by log-rank test. Statistical significance was set at $P < 0.05$.

3. Results

3.1 HSPB1 expression is up-regulated in cardiomyocytes in response to MI

To investigate the possible involvement of HSPB1 in myocardial healing post-MI, we first examined whether cardiac HSPB1 expression is affected by MI. A significant up-regulation of HSPB1 was observed in the myocardium at both the mRNA (11.3 ± 6.4 vs. 1.0 ± 0.3, $P < 0.01$) and protein levels (2.3 ± 0.5 vs. 1.0 ± 0.2, $P < 0.01$) at 24 h after MI, compared with the sham controls (*Figure 1A* and *B*). HSPB1 remained up-regulated at 7 days post-MI (4.2 ± 1.9 vs. 1.0 ± 0.2, $P < 0.01$), and HSPB1 expression was most evident in the cardiomyocytes of the infarct border (*Figure 1B* and *C*). Notably, *in vitro* experiments showed an increase in *Hspb1* mRNA in primary cardiomyocytes exposed to simulated ischaemia by deprivation of glucose and oxygen (referred to as hypoxia hereafter; 1.8 ± 0.6 vs. 1.0 ± 0.2, $P < 0.05$, *Figure 1A*). Together, these findings indicate an up-regulation of HSPB1 in cardiomyocytes in response to MI.

3.2 Generation of cardiomyocyte-specific HSPB1 knockout (*Hspb1*$^{-/-}$) mice

The up-regulation of HSPB1 in cardiomyocytes after MI prompted us to investigate its functional requirement during post-infarct healing. We, therefore, generated cardiomyocyte-specific HSPB1 knockout (*Hspb1*$^{-/-}$) mice. The strategy for generating *Hspb1*$^{-/-}$ mice is shown in *Figure 2A* and Supplementary material online, Figure S1A. The specific knockout of HSPB1 in cardiomyocytes was verified by the absence of HSPB1 protein in the myocardium and in isolated adult cardiomyocytes from *Hspb1*$^{-/-}$ mice (*Figure 2B* and *C*). No effects of HSPB1 deficiency on the expression of other small heat shock proteins, such as HSP22 and HSP32, were observed (see Supplementary material online, Figure S1B). Compared with WT littermates, *Hspb1*$^{-/-}$ mice showed normal body weights, longevity, and reproductive patterns (see Supplementary material online, Figure S1C–E).

3.3 Cardiomyocyte-specific deficiency of HSPB1 increases mortality and ventricular rupture after MI

MI was next induced in WT and *Hspb1*$^{-/-}$ mice, and the mice were followed for 21 days to assess the functional significance of HSPB1 expression during post-MI healing. Strikingly, deficiency of cardiomyocyte HSPB1 increased the mortality after MI by 46.9% [16/23 (69.6%) vs. 5/22 (22.7%), *Figure 2D*, $P < 0.01$]. Necropsies revealed 50.7% more ventricular ruptures in *Hspb1*$^{-/-}$ mice (15/22, 68.1%) than in WT mice (4/23, 17.4%) within 7 days after MI (*Figure 2E* and *F*, $P < 0.01$). No further deaths were observed in either of the two groups between days 8 and 21 after MI.

3.4 Cardiomyocyte-specific deficiency of HSPB1 enlarges infarct size

The infarct sizes were 40.4% ± 2.5% and 56.1% ± 3.7% in WT and *Hspb1*$^{-/-}$ mice, respectively, 24 h after MI (*Figure 3A*). Therefore, the infarcts in *Hspb1*$^{-/-}$ mice were 38.9% larger than in WT mice ($P < 0.01$). The areas at ischaemic risk were comparable between the two groups (see Supplementary material online, Figure S2).

3.5 Cardiomyocyte-specific deficiency of HSPB1 worsens cardiac dysfunction and promotes adverse remodelling after MI

Cardiac function and remodelling were examined serially on days 1, 3, and 7 after MI by echocardiography (*Figure 3B*). Sham mice served as basal controls, and no differences were observed between the two genotypes. However, after MI, *Hspb1*$^{-/-}$ mice showed significantly worse cardiac function, as indicated by decreases in the ejection fraction (EF), fractional shortening (FS), and stroke volume, compared with time-matched WT controls ($P < 0.01$ or 0.05).

Cardiac remodelling is reflected by changes in the left ventricular (LV) diameter and wall thickness (*Figure 3B*). *Hspb1*$^{-/-}$ mice exhibited promoted adverse remodelling, as shown by LV enlargement (increases in LV internal diameter at diastolic phase, LV internal diameter at systolic phase, LV end-diastolic volume, and LV end-systolic volume) and wall thinning (decreases in interventricular septal thickness at diastolic phase, interventricular septal thickness at systolic phase, LV posterior wall thickness at diastolic phase and LV posterior wall thickness at systolic phase) compared with the time-matched WT controls ($P < 0.01$ or 0.05).

3.6 Cardiomyocyte-specific deficiency of HSPB1 suppresses angiogenesis and collagen deposition but increases proteolytic activity after MI

Angiogenesis and ECM remodelling are critical for post-infarct repair.[22–24] Immunostaining for CD31 revealed a significantly reduced capillary density in *Hspb1*$^{-/-}$ infarcts compared with WT controls 7 days after MI (*Figure 4A*, $P < 0.01$). No significant difference in capillary density was detected between sham-operated mice of the two genotypes (see Supplementary material online, Figure S3). ECM formation was also suppressed in *Hspb1*$^{-/-}$ hearts after MI, as indicated by decreased collagen I and III expression (*Figure 4B*, $P < 0.01$) and reduced collagen fibre formation (*Figure 4C*) and maturation (*Figure 4D*), compared with WT controls. In striking contrast, *Hspb1*$^{-/-}$ hearts showed a marked increase in MMP2 and MMP9 activity compared with WT controls after MI, as indicated by zymography (*Figure 4E*). *Hspb1*$^{-/-}$ mice also showed decreased protein expression of α-smooth muscle actin (a marker of fibroblast activation) and N-cadherin (a marker of intercellular integrity) compared with WT controls after MI (see Supplementary material online, Figure S4).

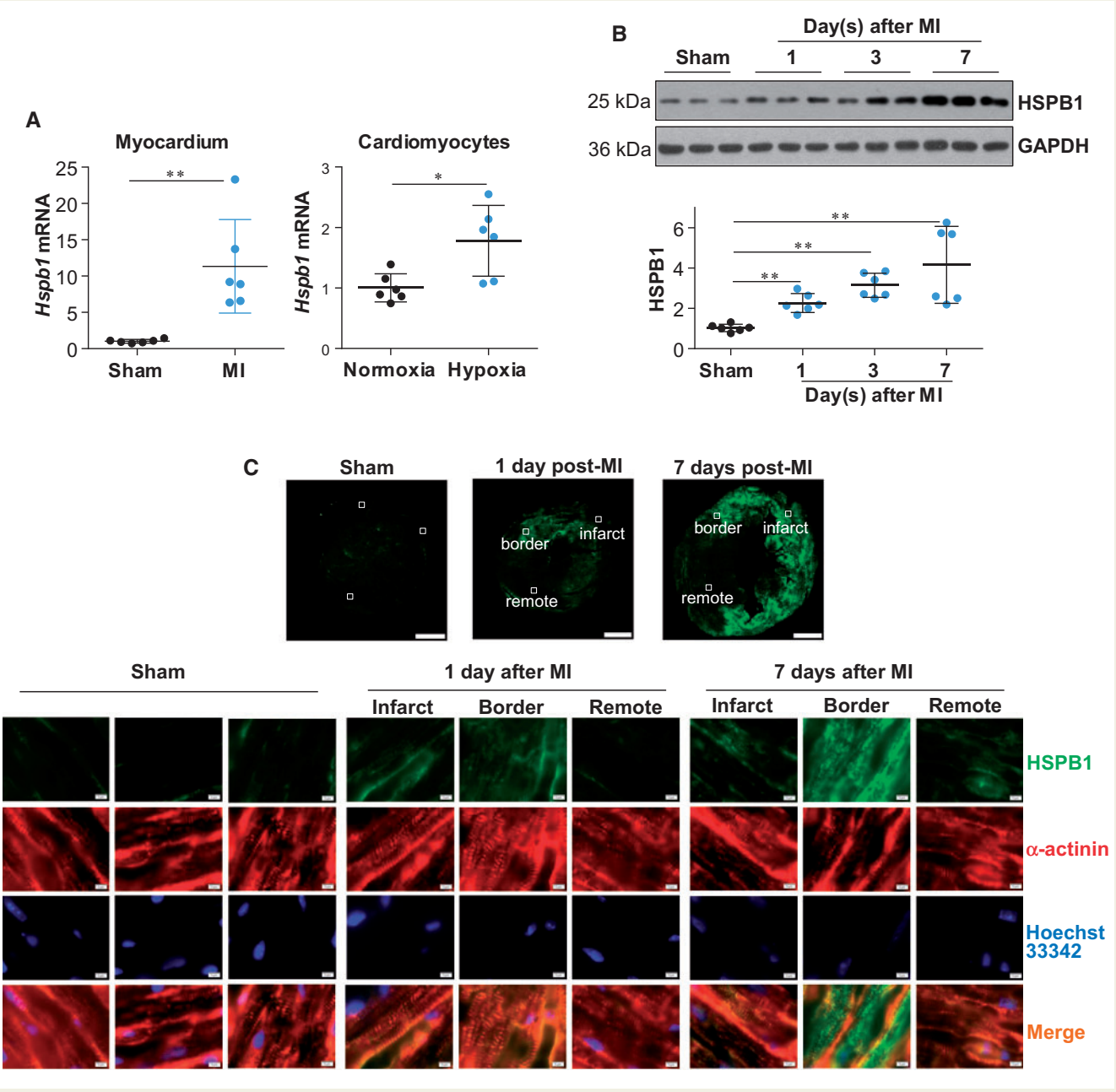

Figure 1 HSPB1 expression was up-regulated in cardiomyocytes in response to MI. (*A*) *Hspb1* mRNA expression. Ventricular tissues were collected 24 h after MI (left panel) and primary cardiomyocytes were harvested 6 h after hypoxia (right panel). Total mRNA was extracted for the analysis of Hspb1 mRNA expression levels. Data were expressed as mean ± SD and analysed using unpaired t-test. $^{**}P < 0.01$, $^{*}P < 0.05$, $n = 6$/group. (*B*) HSPB1 protein expression (immunoblotting). Ventricular tissues were harvested after MI for the indicated times for immunoblotting analysis. Data were expressed as mean ± SD and analysed using one-way ANOVA followed by *post hoc* test. $^{**}P < 0.01$, $n = 6$/group. (*C*) HSPB1 protein expression (immunostaining). Ventricular tissues at the papillary muscles level were collected after MI for the indicated times. Cryosections were prepared for immunofluorescence staining against HSPB1 (green). Alpha-actinin was used to stain cardiomyocytes (red). Hoechst 33342 reagent was used to counterstain the nuclei (blue). The representative images were from six independent experiments. Scale bars, 1mm for upper panel and 10 μm for down panel.

3.7 Cardiomyocyte-specific deficiency of HSPB1 aggravates early myocardial inflammation after MI

Inflammation is an early post-MI response, but excessive inflammation impairs post-MI recovery via multiple mechanisms including disruption of ECM and angiogenesis.[23] Neutrophil infiltration was increased after MI, peaking at 24 h and declining thereafter in WT infarcts (*Figure 5A*). However, the MI-induced neutrophil infiltration was markedly higher in *Hspb1*$^{-/-}$ infarcts at days 1, 3, and 7 post-MI than in the time-matched WT controls. Notably, by day 7 post-MI, neutrophil infiltration had

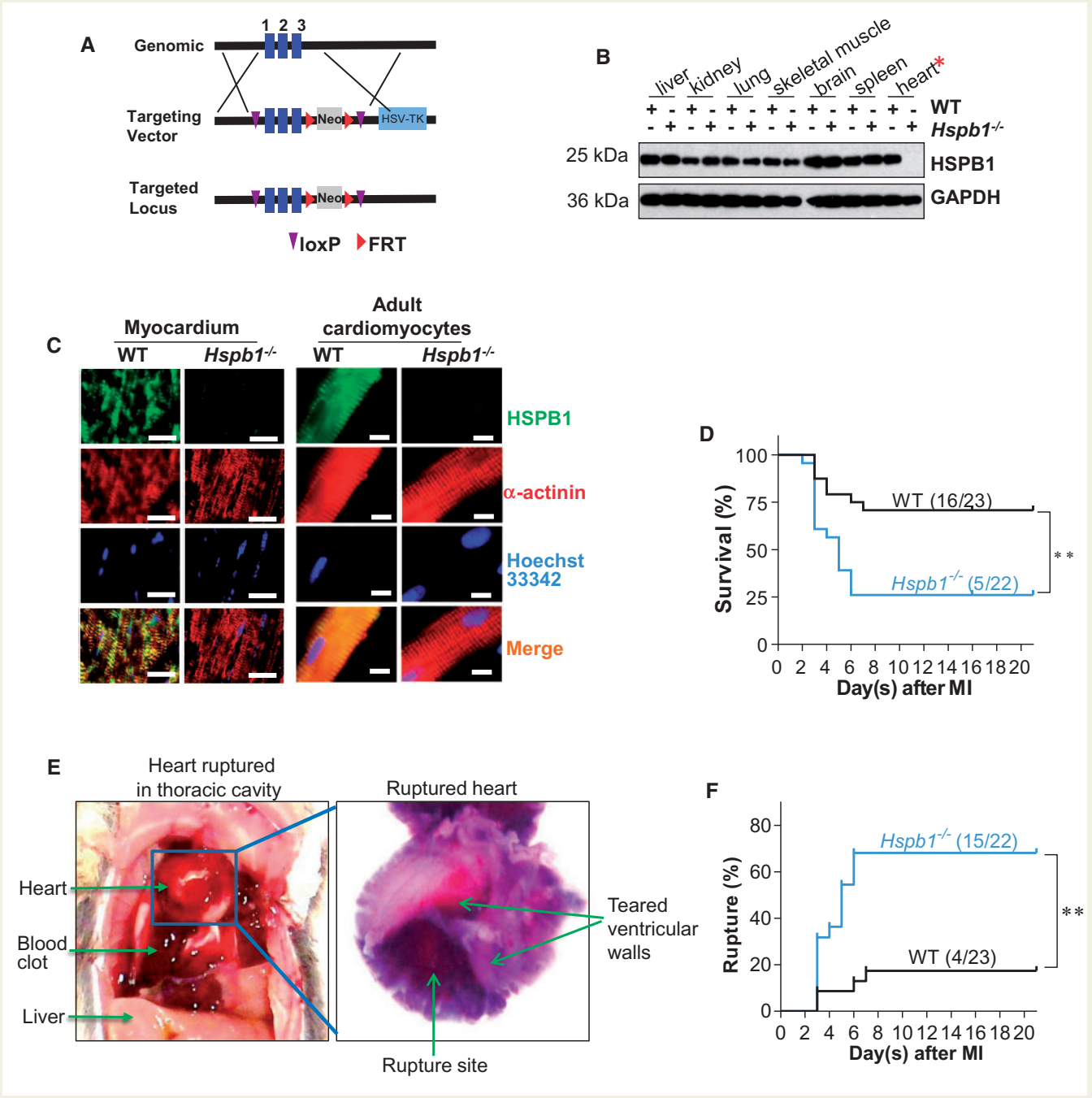

Figure 2 *Hspb1*$^{-/-}$ mice showed increased cardiac rupture and mortality after MI. (*A*) Strategy for creating HSPB1 conditional mice using *loxP* recombinant system. (*B*) Deletion of HSPB1 in *Hspb1*$^{-/-}$ hearts. Different tissues were collected from 8-week-old WT and *Hspb1*$^{-/-}$ mice. HSPB1 protein expression was analysed using immunoblotting. Note that HSPB1 was absent in *Hspb1*$^{-/-}$ hearts. $n = 6$/group. (*C*) Deletion of HSPB1 in cardiomyocytes of *Hspb1*$^{-/-}$ mice. Ventricular tissues (left panel) or isolated adult cardiomyocytes (right panel) were collected from 8-week-old WT and *Hspb1*$^{-/-}$ mice. Immunostaining against HSPB1 (green) was performed. Alpha-actinin was used to stain cardiomyocytes (red). Hoechst 33342 reagent was used to counterstain the nuclei (blue). Note that HSPB1 expression was absent in cardiomyocytes of *Hspb1*$^{-/-}$ mice. Scale bars, 10 μm. $n = 6$/group. (*D*) Kaplan–Meier survival curves. *Hspb1*$^{-/-}$ and WT mice were subjected to MI insult. Mice survival was recorded within 21 day post-MI. $^{**}P < 0.01$ analysed by log-rank test. $n = 22$–23 per group. (*E* and *F*) Cardiac rupture. Autopsy was performed in MI-induced death of mice. Cardiac rupture was characterized by presence of intrathoracic blood clots (left panel, *E*) and perforation on the infarcted wall (right panel, *E*). Note that a significant more incidence of cardiac rupture was detected in *Hspb1*$^{-/-}$ mice after MI (*F*). $^{**}P < 0.01$ analysed by log-rank test. $n = 22$–23 per group.

returned to the basal level in WT mice but remained elevated in *Hspb1*$^{-/-}$ infarcts compared with sham controls. Similarly, *Hspb1*$^{-/-}$ hearts showed significantly more macrophage infiltration than WT controls on day 3 after MI (*Figure 5B*).

Consistent with the increased infiltration by neutrophils/macrophages, mRNA levels of inflammatory mediators (*Il-1β*, *Il-8*, *Il-6*, and *Icam-1*) were increased in *Hspb1*$^{-/-}$ mice compared with WT mice after MI (*Figure 5C*). However, these mediators might not be derived fro

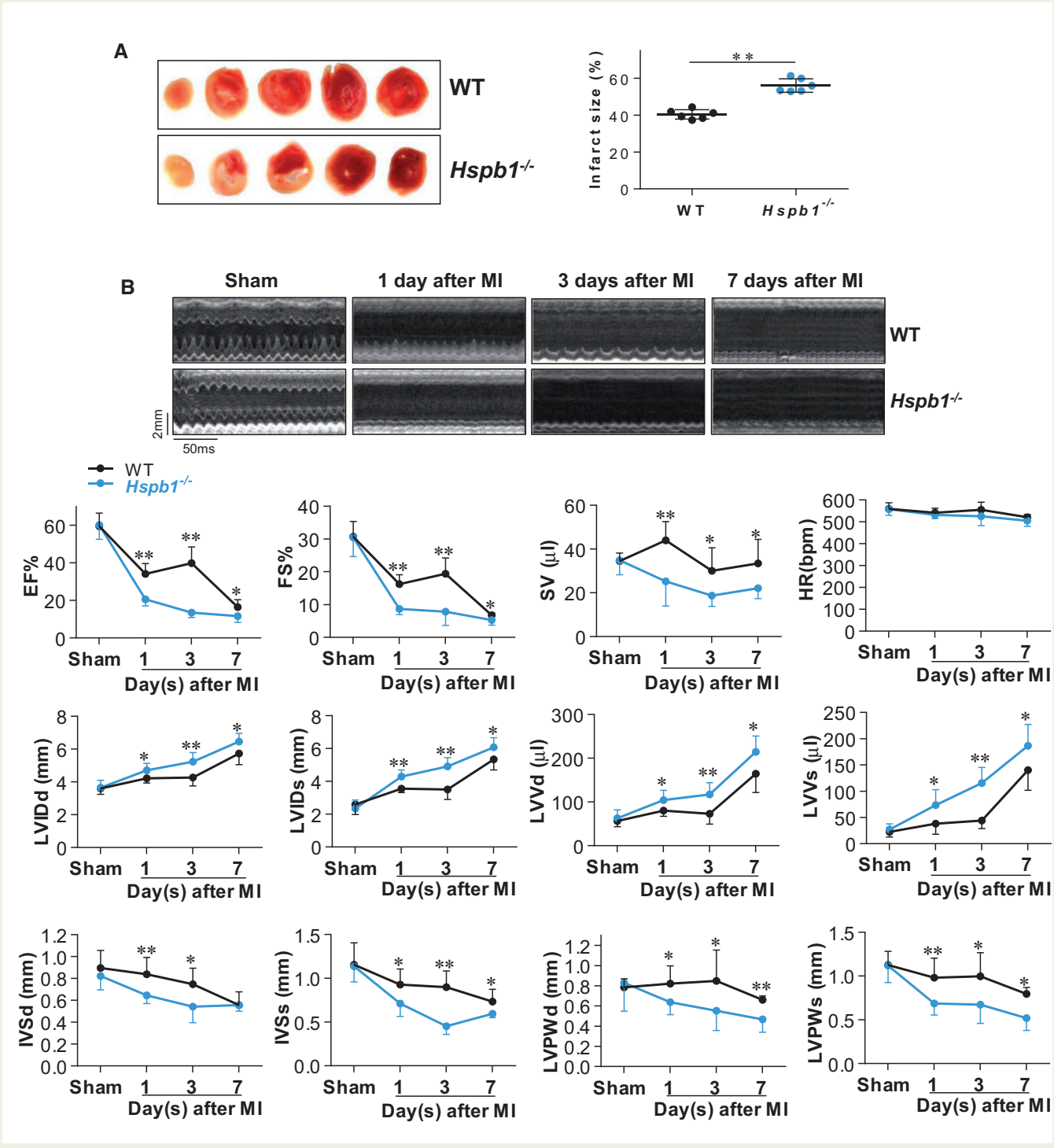

Figure 3 Deficiency of HSPB1 enlarged infarct size and worsened cardiac dysfunction and remodelling. (*A*) Infarct size. Infarct size was evaluated by TTC staining 24 h post-MI. The red area resembled the vital myocardium and the white area indicated the infarct. Data were expressed as mean ± SD and analysed using unpaired *t*-test. $^{**}P < 0.01$, $n = 6$/group. (*B*) Cardiac dysfunction and remodelling. Cardiac function and remodelling was examined serially using 2D echocardiography. The representative M-mode images at the papillary muscles were shown in upper panel. Parameters were obtained from M-mode tracings and averaged using three to five cardiac cycles. Data were expressed as mean ± SD and analysed using two-way ANOVA analysis followed by *post hoc* test. $^{**}P < 0.01$ and $^{*}P < 0.05$ vs. the time-matched WT mice, $n = 8$ for all the groups except for $n = 6$ in *Hspb1*$^{-/-}$ mice with MI for 7 days. Time stamp and scale bar of M-mode images were shown in the figure. EF (%), ejection fraction; FS (%), fractional shortening; SV (μL), stroke volume; HR (b.p.m.), heart rate; LVIDd (mm), left ventricular internal diameter at diastolic phase; LVIDs (mm), left ventricular internal diameter at systolic phase; LVVd (μL), left ventricular end-diastolic volume; LVVs (μL), left ventricular end-systolic volume; IVSd (mm), interventricular septal thickness at diastolic phase; IVSs (mm), interventricular septal thickness at systolic phase; LVPWd (mm), left ventricular posterior wall thickness at diastolic phase; LVPWs (mm), left ventricular posterior wall thickness at systolic phase.

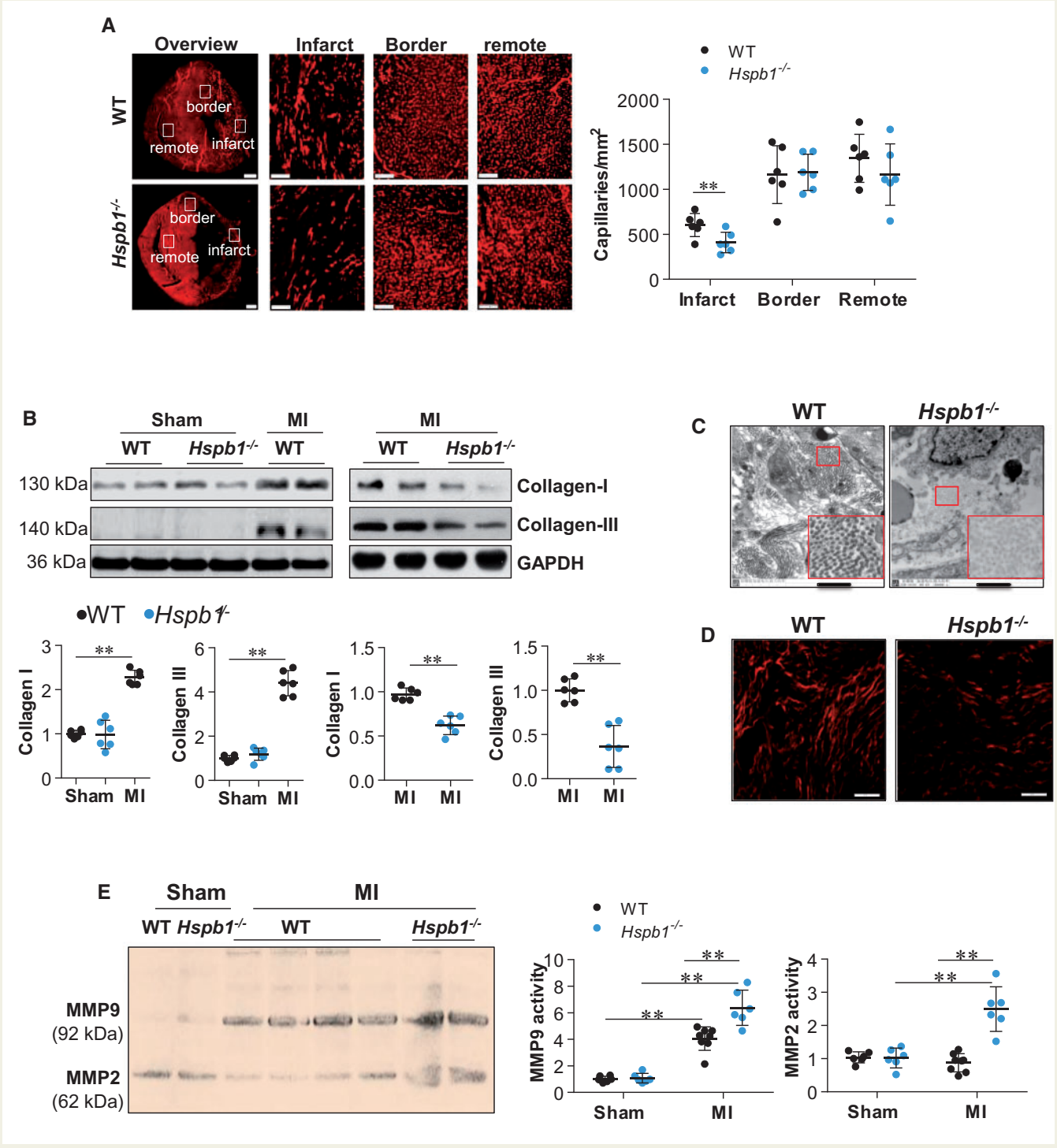

Figure 4 Deficiency of HSPB1 suppressed angiogenesis and ECM remodelling after MI. (*A*) Angiogenesis. Ventricular tissues at the papillary muscles level were collected after MI for 7 days. Cryosections were prepared for immunofluorescence staining against CD31. The representative images were from six independent experiments. Scale bars, 500 μm for the overview images and 100 μm for the infarct, border and remote images. Data were expressed as mean ± SD and analysed using unpaired *t*-test. $^{**}P < 0.01$, $n = 6$/group. (*B*) Collagen expression. Ventricular tissues were collected 24 h after MI for immunoblotting with the indicated antibodies. Data were expressed as mean ± SD and analysed using two-way ANOVA followed by *post hoc* test. $^{**}P < 0.01$, $n = 6$/group. (*C*) Collagen fibre formation. Ventricular tissues were collected 3 days after MI for electron microscope analysis. Scale bars, 1 μm, $n = 6$/group. (*D*) ECM maturation. Ventricular tissues were collected 7 days after MI. Paraffin-embedded sections were prepared and stained with Sirius red and analysed with polarized light microscopy at a magnification of ×400. $n = 6$/group. Scale bars, 50 μm. (*E*) MMPs activation. Ventricular tissues were collected 24 h after MI for zymography analysis. Data were expressed as mean ± SD and analysed using two-way ANOVA followed by *post hoc* test. $^{**}P < 0.01$, $n = 6$–8/group.

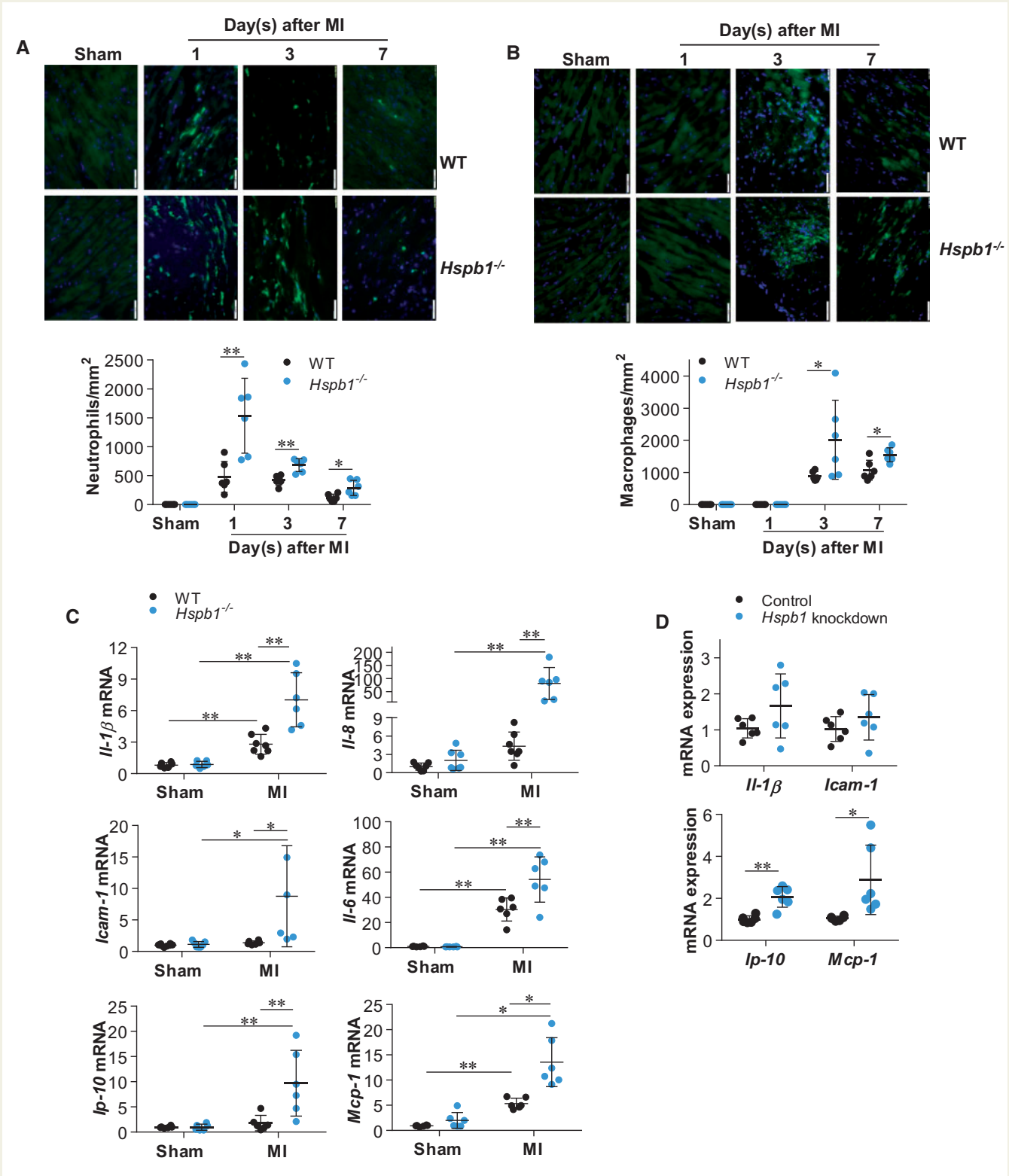

Figure 5 Deficiency of HSPB1 enhanced the MI-induced inflammatory responses and chemokine induction in cardiomyocytes. (*A* and *B*) Leucocyte recruitment. Ventricular tissues at the papillary muscles level were collected after MI for the indicated times. Cryosections were prepared for immunofluorescence staining against neutrophil (*A*) or F4/80 (*B*) (green). Hoechst 33342 reagent was used to counterstain the nuclei (blue). Data were expressed as mean ± SD and analysed using unpaired *t*-test. $*P < 0.05$, $**P < 0.01$, $n = 6$/group. Scale bars, 50 μm. (*C*) Cytokines and chemokines in myocardium. Ventricular tissues were collected 24 h post-MI for mRNA analysis. Data were expressed as mean ± SD and analysed using two-way ANOVA followed by *post hoc* test. $**P < 0.01$ and $*P < 0.05$, $n = 6$–8 per group. (*D*) Cytokines and chemokines in cardiomyocytes. Primary cardiomyocytes were transfected with *Hspb1* siRNA to knock down HSPB1 expression. Cardiomyocytes transfected with scramble RNA served as controls. Following hypoxia for 6 h, cardiomyocytes were harvested for mRNA analysis. Data were expressed as mean ± SD and analysed using unpaired t-tests. $**P < 0.01$ and $*P < 0.05$, $n = 6$/group.

cardiomyocytes within *Hspb1*$^{-/-}$ hearts, as their expression in primary cardiomyocytes was not affected by *Hspb1* knockdown under hypoxic conditions (*Figure 5D* and Supplementary material online, Figure S5). The expression of *Il-10* mRNA was comparable between the two genotypes after MI (see Supplementary material online, Figure S6).

3.8 HSPB1 deficiency augments chemokine induction in cardiomyocytes after MI

Locally secreted chemokines attract and recruit leucocytes into the myocardium after MI. Although mRNA levels of the chemokines *Gro-α*, *Gro-β*, *Gro-γ*, and *Ena78* were not significantly different between the two genotypes after MI (see Supplementary material online, Figure S7), the expression of the chemokines *Ip-10* and *Mcp-1* was markedly increased in *Hspb1*$^{-/-}$ hearts compared with WT controls (*Figure 5C*). Notably, the increase of *Ip-10* and *Mcp-1* in *Hspb1*$^{-/-}$ infarcts could be attributed to *Hspb1*$^{-/-}$ cardiomyocytes, because *Hspb1* knockdown markedly increased the expression of these chemokines in primary cardiomyocytes under hypoxia *in vitro* (*Figure 5D*). The data suggest that HSPB1 acts as a negative regulator of chemokine induction in cardiomyocytes under ischaemic conditions.

3.9 HSPB1 regulates chemokine expression in cardiomyocytes by modulating TLR4/MyD88/NFκB signalling

3.9.1 HSPB1 deficiency activates NFκB

NFκB plays a pivotal role in inducing chemokine expression.[25] We, therefore, evaluated NFκB activation by examining the nuclear translocation of its p65 subunit. No difference in cytosolic NFκB content was observed between the two genotypes after MI (*Figure 6A*). However, by immunoblotting and immunofluorescence, a marked enhancement of MI-induced nuclear translocation of NFκB was detected in *Hspb1*$^{-/-}$ hearts compared with WT controls (*Figure 6A* and Supplementary material online, Figure S8). These increases in NFκB expression and nuclear translocation in *Hspb1*$^{-/-}$ MI hearts could be attributed to *Hspb1*$^{-/-}$ cardiomyocytes, because knockdown of *Hspb1* in primary cardiomyocytes enhanced NFκB expression and nuclear translocation under hypoxic conditions *in vitro* (*Figure 6B* and *C*).

3.9.2 HSPB1 deficiency enhances TLR4/MyD88/NFκB signalling

Increases in TLR4 and MyD88 expression were observed in *Hspb1*$^{-/-}$ hearts compared with WT hearts after MI (*Figure 6D*). IκBα, a downstream target of TLR4/MyD88 that directly prevents NFκB nuclear translocation, was more highly phosphorylated in *Hspb1*$^{-/-}$ hearts than in WT controls after MI. Knockdown of *Hspb1* in primary cardiomyocytes also increased the expression of *Tlr4, Myd88, and Nfκb* mRNA under hypoxic conditions *in vitro* (*Figure 6B* and *E*), suggesting that HSPB1 acts as a negative regulator of TLR4/MyD88/NFκB signalling in cardiomyocytes within MI hearts.

3.9.3 NFκB mediates the enhanced chemokine induction observed in *Hspb1*$^{-/-}$ cardiomyocytes

To investigate whether TLR4/MyD88/NFκB signalling mediates the enhanced chemokine induction in *Hspb1*$^{-/-}$ cardiomyocytes post-MI, primary cardiomyocytes were treated with PDTC, a widely used NFκB inhibitor.[26,27] PDTC abolished the enhancement of NFκB nuclear translocation and chemokines (*Ip-10* and *Mcp-1*) induction in *Hspb1 knockdown* cardiomyocytes under hypoxic conditions (*Figure 7A* and Supplementary material online, Figure S9). QNZ (EVP4593), another NFκB inhibitor, also abrogated the effect of *Hspb1* knockdown on the hypoxia-induced expression of *Ip-10* and *Mcp-1* in primary cardiomyocytes *in vitro* (see Supplementary material online, Figure S10A and *B*). These data suggest that HSPB1 regulates chemokine expression in cardiomyocytes by modulating NFκB signalling under ischaemic conditions.

3.10 NFκB mediates the HSPB1 deficiency-induced aggravation of post-MI inflammation

We next examined whether NFκB activation mediates the HSPB1 deficiency-induced aggravation of post-MI inflammation. Notably, PDTC also prevented the enhanced neutrophil recruitment in *Hspb1*$^{-/-}$ hearts 24 h after MI (*Figure 7B* and Supplementary material online, Figure S11). In the presence of PDTC, *Hspb1*$^{-/-}$ hearts showed no difference in neutrophil recruitment from WT controls after MI.

3.11 NFκB mediates the HSPB1 deficiency-induced aggravation of cardiac dysfunction after MI

PDTC administration markedly increased EF and FS in both WT and *Hspb1*$^{-/-}$ mice 24 h after MI (*Figure 7C*). In the presence of PDTC, no significant difference in EF or FS was observed between *Hspb1*$^{-/-}$ and WT mice at 1, 3, 7, 14 and 21 days after MI (*Figure 7C* and Supplementary material online, Figure S12).

3.12 NFκB mediates the HSPB1 deficiency-induced exacerbation of ventricular rupture and mortality after MI

PDTC administration markedly reduced mortality in both genotypes within 21 days after MI (*Figure 7D*). PDTC also reduced the incidence of cardiac rupture in both genotypes after MI (*Figure 7E*). After treatment with PDTC, *Hspb1*$^{-/-}$ mice showed no difference in mortality or cardiac rupture compared with WT mice after MI (*Figure 7D* and *E*).

4. Discussion

The significant finding of this study is that MI up-regulated HSPB1 expression in cardiomyocytes, while cardiomyocyte-specific deficiency of HSPB1 promoted adverse remodelling following MI, resulting in increased cardiac dysfunction, cardiac rupture, and mortality. This action of cardiomyocyte HSPB1 was due, at least in part, to modulation of the inflammatory response in a NFκB-dependent manner. Our data suggest that cardiomyocyte HSPB1 acts as a negative regulator of inflammation and plays an essential role in repairing tissue damage after MI.

Cardiac rupture is a severe and potentially fatal complication of MI.[28] Survival is poor in MI patients who have suffered cardiac rupture, with an in-hospital mortality of 60–90% for LV free wall rupture and 30–50% for ventricular septum rupture.[6] There is no effective therapy for this complication.[6,28] Based on Becker's classification, acute ruptures occur within 48 h after MI and subacute ruptures occur within 3–10 days after MI in human patients.[6] Although it remains unclear if this classification is also applicable to the mouse model of MI, we did find that deficiency of HSPB1 in cardiomyocytes markedly increased the frequency of MI-induced cardiac rupture, and all the cardiac ruptures occurred within

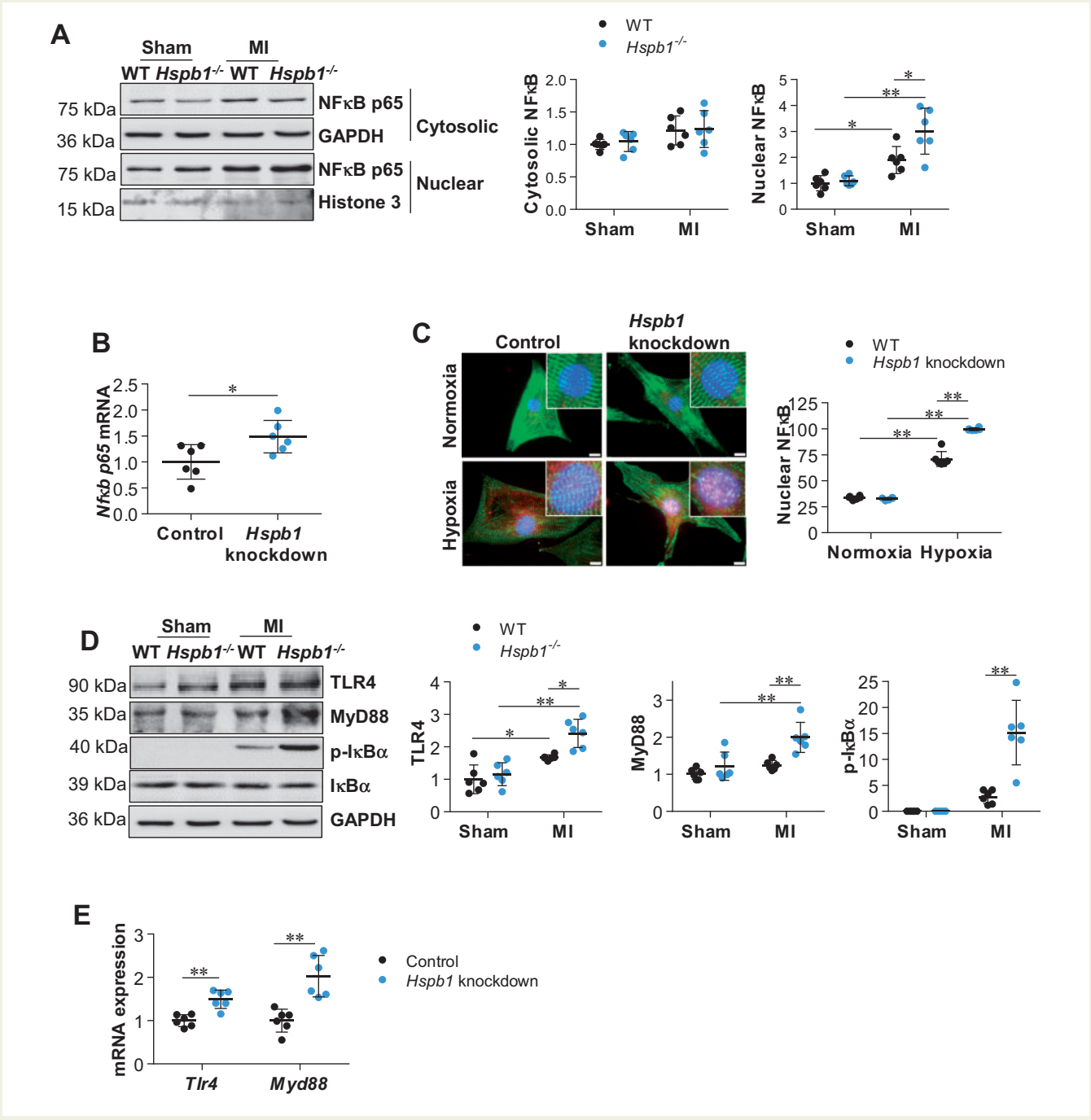

Figure 6 Deficiency of HSPB1 augmented the MI-induced NFκB activation in cardiomyocytes. (*A*) NFκB p65 nuclear translocation in myocardium. Ventricular tissues were collected 24 h post-MI. Cytosolic and nuclear protein fractions were prepared for immunoblotting against NFκB p65 subunit. Data were expressed as mean ± SD and analysed using two-way ANOVA followed by *post hoc* test. $^{**}P < 0.01$, $^{*}P < 0.05$, $n = 6$/group. (*B*) *Nfκb p65* mRNA expression in primary cardiomyocytes. Following hypoxia for 6 h, cardiomyocytes were harvested for analysing *Nfκb p65* mRNA levels. Data were expressed as mean ± SD and analysed using unpaired *t*-tests. $^{*}P < 0.05$, $n = 6$/group. (*C*) NFκB p65 nuclear translocation in primary cardiomyocytes. Following hypoxia for 6 h, cardiomyocytes were harvested for immunostaining against NFκB p65 (red). Alpha-actinin was used to stain cardiomyocytes (green). Hoechst 33342 reagent was used to counterstain the nuclei (blue). Scale bars, 10 μm. Data were expressed as mean ± SD and analysed using two-way ANOVA followed by *post hoc* test. $^{**}P < 0.01$, $n = 6$/group. (*D*) TLR4/MyD88 signalling in myocardium. Ventricular tissues were collected 24 h post-MI for immunoblotting analysis. Data were expressed as mean ± SD and analysed using two-way ANOVA followed by *post hoc* test. $^{**}P < 0.01$, $^{*}P < 0.05$, $n = 6$/group. (*E*) TLR4/MyD88 signalling in cardiomyocytes. Following hypoxia for 6 h, cardiomyocytes were harvested for mRNA analysis. Data were expressed as mean ± SD and analysed using unpaired *t*-test. $^{**}P < 0.01$, $n = 6$/group.

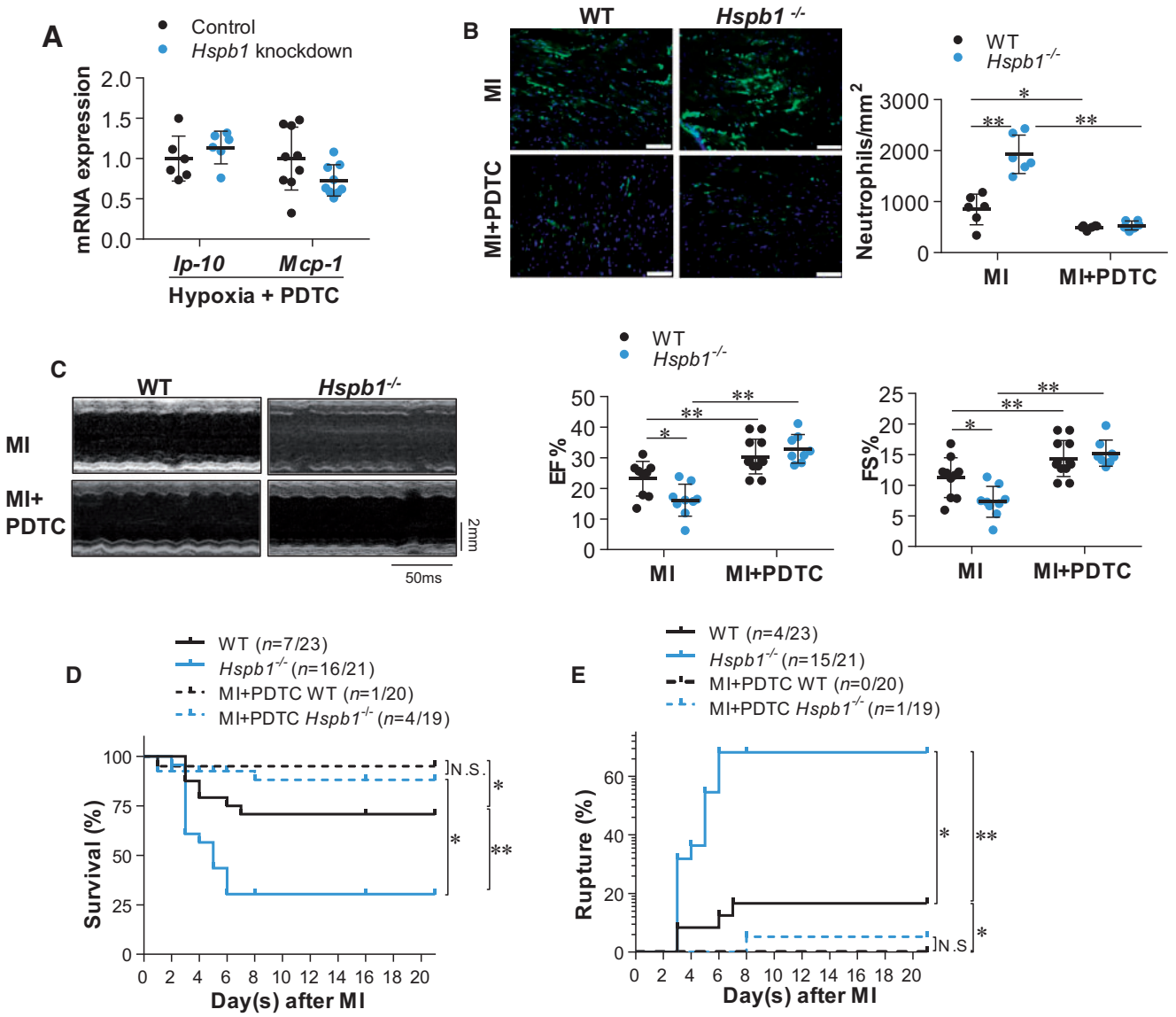

Figure 7 Inhibition of NFκB reversed the HSPB1 deficiency-induced exaggeration of cardiac damages after MI. (*A*) Chemokine expression in cardiomyocytes. Cardiomyocytes were exposed to hypoxia for 6 h in the presence of PDTC. Levels of mRNA were examined. Data were expressed as mean ± SD and analysed using unpaired *t*-test. $n = 6–9$/group. (*B*) Neutrophil infiltration in myocardium. Ventricular tissues at the papillary muscles level were collected at 24 h post-MI in the presence or absence of PDTC. Cryosections were prepared for immunofluorescence staining against neutrophil (green). Hoechst 33342 reagent was used to counterstain the nuclei (blue). Data were expressed as mean ± SD and analysed using two-way ANOVA followed by *post hoc* test. Scale bars, 50 μm; $^{**}P < 0.01$ or $^{*}P < 0.05$, $n = 6$/group. (*C*) Cardiac function. Cardiac function was evaluated using echocardiography 24 h post-MI in the presence or absence of PDTC. Data were expressed as mean ± SD and analysed using two-way ANOVA followed by *post hoc* test. Time stamp and scale bar of M-mode images were shown in the figure. $^{**}P < 0.01$ or $^{*}P < 0.05$, $n = 8–12$/group. (*D*) Kaplan–Meier survival curves. Mice survival was recorded within 21 day post-MI in the presence or absence of PDTC. $^{**}P < 0.01$ or $^{*}P < 0.05$ analysed using log-rank test. $n = 19–23$/group. N.S., no significance. (*E*) Cardiac rupture. Autopsy was performed to examine cardiac rupture in MI-induced death of mice in the presence or absence of PDTC. $^{**}P < 0.01$ or $^{*}P < 0.05$ analysed using log-rank test. $n = 19–23$/group. N.S., no significance.

3–7 days post-MI. Clinical and experimental evidence demonstrates that subacute cardiac rupture results from progressive thinning and expansion of the infarct ventricular wall.[6,29] Indeed, we observed that MI-induced wall thinning and chamber enlargement were exacerbated in *Hspb1*$^{-/-}$ mice, suggesting that HSPB1 within cardiomyocytes plays an important role in limiting adverse remodelling and preventing cardiac rupture following MI.

MI triggers an intense inflammatory response in the myocardium that is characterized by recruitment of neutrophils, macrophages, and monocytes.[6] These leucocytes promote repairment of infarcted hearts by phagocytizing dead tissue and providing growth factors that support angiogenesis and ECM synthesis.[30] However, they also release inflammatory mediators, such as cytokines and reactive oxygen species, which damage nearby cardiomyocytes that survived the ischaemic injury.

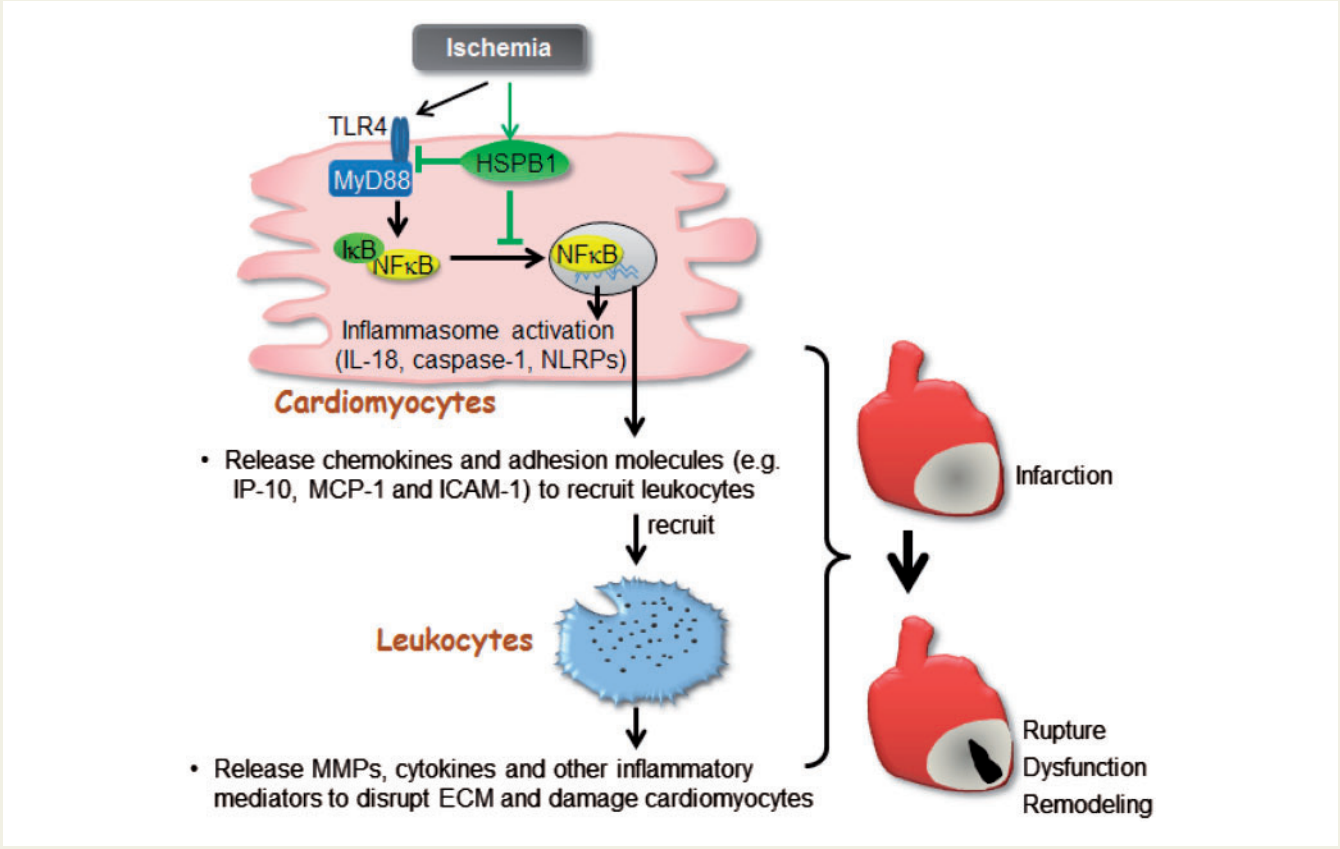

Figure 8 Scheme represents that Cardiomyocyte-HSPB1 acts as a negatively regulator of NFκB-dependent inflammatory responses and plays essential role in wound healing after MI. In infarcted myocardium, cardiomyocyte TLR4/MyD88 was activated, and IκBα was phosphorylated and degraded, leading to NFκB nuclear translocation to stimulate the expression of inflammatory mediators including chemokines, cellular adhesion molecules, and the genes related to inflammasome activation. The chemokines and adhesion molecules from cardiomyocytes recruit leucocytes into infarcted myocardium to evoke inflammatory injury. HSPB1 was up-regulated in cardiomyocytes in response to MI, while knockout of cardiomyocyte-HSPB1 exaggerated the NFκB-dependent induction of chemokines for further leucocyte recruitment that leading to excessive inflammation, and ultimately caused cardiac rupture and worsened cardiac dysfunction following MI. cardiomyocyte HSPB1 is a negative regulator of NFκB proinflammatory signalling and plays an essential role in wound healing after MI.

Matrix metalloproteinases released from leucocytes will disrupt ECM remodelling after MI. The risk of rupture correlates with the magnitude of inflammatory cell infiltration.[6,24,30] Global deletion of matrix metalloproteinases such as MMP28 prevents cardiac rupture after MI,[31] while increased leucocyte recruitment and activation caused by global growth/differentiation factor 15 deficiency increases cardiac rupture after MI.[31,32] Interestingly, we observed that cardiomyocyte-specific deletion of HSPB1 increased the magnitude and duration of MI-induced recruitment of neutrophils and macrophages. Recent evidence suggests an innate immune pathway known as the 'inflammasomes' during MI injury. The formation of the inflammasome results in additional impairment of functional myocardium and adverse cardiac remodelling after MI, leading to HF.[33,34] The inflammasome is a large multiprotein complex that is formed in the cytosol in response to danger signals released by dying cardiomyocytes and degraded ECM.[34,35] Most inflammasomes typically contain one of the NLR family proteins (NLRP1, NLRP3, NLRP6, NLRP7, NLRP12, and NLRC4), apoptosis-associated speck-like protein containing a caspase recruitment domain. Investigations demonstrate that inflammasomes drive expression of certain inflammatory expression mediators such as IL-1β, that serve as early and prominent mediators for inflammatory responses after MI. Inhibiting inflammasome formation limits infarct size and cardiac remodelling after MI.[33,36] Interestingly, the MI-induced up-regulation of cytokines and genes related to inflammasome signalling (see Supplementary material online, Figure S13) was augmented in *Hspb1*$^{-/-}$ mice. Taken together, our data suggest a cardiomyocyte-specific role for HSPB1 in the recruitment of leucocytes in MI hearts. These augmented inflammatory responses promote adverse remodelling, impair cardiac function, and increase the risk of cardiac rupture in *Hspb1*$^{-/-}$ mice post-MI.

Locally secreted chemokines are critical in attracting and recruiting leucocytes into the myocardium after MI, and NFκB plays a pivotal role in numerous aspects of the inflammatory response, including chemokine expression.[6,37] Indeed, NFκB inhibition has been shown to decrease the expression of chemokines and cytokines, attenuate cardiac dysfunction and remodelling, decrease the risk of cardiac rupture, and improve the survival of mice post-MI.[11,38] Interestingly, we observed that *Hspb1*$^{-/-}$ hearts showed increased activation of NFκB and increased expression of the chemokines IP-10 and MCP-1 post-MI, and *in vitro* experiments with primary cardiomyocytes confirmed that these chemokines were attributed to *Hspb1*$^{-/-}$ cardiomyocytes. After inhibiting NFκB activity with PDTC, a widely used NFκB inhibitor,[26,27] the HSPB1 knockdown-induced increase in chemokine expression in hypoxic cardiomyocytes

and the HSPB1 deficiency-induced increase in leucocyte infiltration of infarcted myocardium were abolished. Importantly, PDTC reversed the HSPB1 deficiency-induced aggravation in cardiac dysfunction, cardiac rupture, and mortality following MI. These data suggest that HSPB1 negatively regulates NFκB-mediated chemokine expression in cardiomyocytes in injured myocardium. This pathway is a crucial mechanism through which cardiomyocytes regulate leucocyte trafficking and the subsequent inflammatory response after MI.

Activation of NFκB mediates the expression of pro-fibrotic factors such as transforming growth factor-β1 that activate fibroblasts. However, NFκB also drives the expression of chemokines and cytokines that recruit inflammatory cells to damaged cardiac tissue after MI. Some of these chemokines such as IP-10, also possess anti-angiogenic and anti-fibrotic properties,[4,7,9] while other proinflammatory mediators such as IL-1β, can inhibit myofibroblast conversion.[39] Additionally, the recruited inflammatory cells release proteinases that degrade ECM. Thus, optimal tissue repair after MI requires a proper physiological balance between the early inflammatory phase and the subsequent reparative phase. In this study, deficiency of HSPB1 in cardiomyocytes magnified and prolonged inflammation after MI in a NFκB-dependent manner.

In consistence with the observation in male mice, HSPB1 deficiency also exaggerated the MI-induced cardiac injury in female mice (see Supplementary material online, Figure S14). Moreover, the myocardial ischaemia/reperfusion injury was exaggerated by HSPB1 deficiency (see Supplementary material online, Figure S15). However, this study has the following major limitations. First, the mechanism through which HSPB1 regulates NFκB activity in cardiomyocytes has not been clarified. Second, it is not known whether fibroblast activation is involved in the effects of cardiomyocyte HSPB1 during post-MI repair. Finally, the role of HSPB1 in the regulation of angiogenesis in MI hearts remains unknown. These questions should be addressed in future studies.

In summary, we provide novel evidence that HSPB1 in cardiomyocytes is involved in cardiac wound healing post-MI. These actions of HSPB1 in cardiomyocytes are mediated, at least in part, through modulation of NFκB-mediated inflammatory responses (*Figure 8*). Targeting HSPB1 expression in cardiomyocytes could be an alternative therapeutic approach for suppressing myocardial inflammation and improving wound healing following MI.

Conflict of interest: none declared.

Funding

This work was supported by the National Natural Science Foundation of China [81770854, 81571378, 81571290, 81370260, 81371450], by Jiangsu Province's Outstanding Medical Academic Leader program (15), by Project Funded by the Priority Academic Program Development of Jiangsu Higher Education Institutions (PAPD), a project funded by Collaborative Innovation Center for Cardiovascular Disease Translational Medicine, and Jiangsu Provincial Key Discipline of Medicine [ZDXKA2016003].

References

1. Benjamin EJ, Blaha MJ, Chiuve SE, Cushman M, Das SR, Deo R, de Ferranti SD, Floyd J, Fornage M, Gillespie C, Isasi CR, Jimenez MC, Jordan LC, Judd SE, Lackland D, Lichtman JH, Lisabeth L, Liu S, Longenecker CT, Mackey RH, Matsushita K, Mozaffarian D, Mussolino ME, Nasir K, Neumar RW, Palaniappan L, Pandey DK, Thiagarajan RR, Reeves MJ, Ritchey M, Rodriguez CJ, Roth GA, Rosamond WD, Sasson C, Towfighi A, Tsao CW, Turner MB, Virani SS, Voeks JH, Willey JZ, Wilkins JT, Wu JH, Alger HM, Wong SS, Muntner P; American Heart Association Statistics Committee and Stroke Statistics Subcommittee. Heart disease and stroke statistics-2017 update: a report from the American Heart Association. *Circulation* 2017;**135**:e146–e603.
2. Nahrendorf M, Hu K, Frantz S, Jaffer FA, Tung CH, Hiller KH, Voll S, Nordbeck P, Sosnovik D, Gattenlohner S, Novikov M, Dickneite G, Reed GL, Jakob P, Rosenzweig A, Bauer WR, Weissleder R, Ertl G. Factor XIII deficiency causes cardiac rupture, impairs wound healing, and aggravates cardiac remodeling in mice with myocardial infarction. *Circulation* 2006;**113**:1196–1202.
3. Prabhu SD, Frangogiannis NG. The biological basis for cardiac repair after myocardial infarction: from inflammation to fibrosis. *Circ Res* 2016;**119**:91–112.
4. Chen B, Frangogiannis NG. Immune cells in repair of the infarcted myocardium. *Microcirculation* 2017;**24**:e12305.
5. Savvatis K, Pappritz K, Becher PM, Lindner D, Zietsch C, Volk HD, Westermann D, Schultheiss HP, Tschope C. Interleukin-23 deficiency leads to impaired wound healing and adverse prognosis after myocardial infarction. *Circ Heart Fail* 2014;**7**:161–171.
6. Gao XM, White DA, Dart AM, Du XJ. Post-infarct cardiac rupture: recent insights on pathogenesis and therapeutic interventions. *Pharmacol Ther* 2012;**134**:156–179.
7. Cavalera M, Frangogiannis NG. Targeting the chemokines in cardiac repair. *Curr Pharm Des* 2014;**20**:1971–1979.
8. Bujak M, Dobaczewski M, Gonzalez-Quesada C, Xia Y, Leucker T, Zymek P, Veeranna V, Tager AM, Luster AD, Frangogiannis NG. Induction of the CXC chemokine interferon-gamma-inducible protein 10 regulates the reparative response following myocardial infarction. *Circ Res* 2009;**105**:973–983.
9. Bodnar RJ, Yates CC, Wells A. IP-10 blocks vascular endothelial growth factor-induced endothelial cell motility and tube formation via inhibition of calpain. *Circ Res* 2006;**98**:617–625.
10. Ma J, Wei M, Wang Q, Li J, Wang H, Liu W, Lacefield JC, Greer PA, Karmazyn M, Fan GC, Peng T. Deficiency of Capn4 gene inhibits nuclear factor-kappaB (NF-kappaB) protein signaling/inflammation and reduces remodeling after myocardial infarction. *J Biol Chem* 2012;**287**:27480–27489.
11. Kawano S, Kubota T, Monden Y, Tsutsumi T, Inoue T, Kawamura N, Tsutsui H, Sunagawa K. Blockade of NF-kappaB improves cardiac function and survival after myocardial infarction. *Am J Physiol Heart Circ Physiol* 2006;**291**:H1337–H1344.
12. Benjamin IJ, McMillan DR. Stress (heat shock) proteins: molecular chaperones in cardiovascular biology and disease. *Circ Res* 1998;**83**:117–132.
13. Seemampillai B, Germack R, Felkin LE, McCormack A, Rose ML. Heat shock protein-27 delays acute rejection after cardiac transplantation: an experimental model. *Transplantation* 2014;**98**:29–38.
14. Narumi T, Shishido T, Otaki Y, Kadowaki S, Honda Y, Funayama A, Honda S, Hasegawa H, Kinoshita D, Yokoyama M, Nishiyama S, Takahashi H, Arimoto T, Miyamoto T, Watanabe T, Tanaka A, Woo CH, Abe J, Takeishi Y, Kubota I. High-mobility group box 1-mediated heat shock protein beta 1 expression attenuates mitochondrial dysfunction and apoptosis. *J Mol Cell Cardiol* 2015;**82**:1–12.
15. Lin S, Wang Y, Zhang X, Kong Q, Li C, Li Y, Ding Z, Liu L. HSP27 alleviates cardiac aging in mice via a mechanism involving antioxidation and mitophagy activation. *Oxid Med Cell Longev* 2016;**2016**:2586706.
16. Efthymiou CA, Mocanu MM, de Belleroche J, Wells DJ, Latchmann DS, Yellon DM. Heat shock protein 27 protects the heart against myocardial infarction. *Basic Res Cardiol* 2004;**99**:392–394.
17. Hollander JM, Martin JL, Belke DD, Scott BT, Swanson E, Krishnamoorthy V, Dillmann WH. Overexpression of wild-type heat shock protein 27 and a nonphosphorylatable heat shock protein 27 mutant protects against ischemia/reperfusion injury in a transgenic mouse model. *Circulation* 2004;**110**:3544–3552.
18. You W, Min X, Zhang X, Qian B, Pang S, Ding Z, Li C, Gao X, Di R, Cheng Y, Liu L. Cardiac-specific expression of heat shock protein 27 attenuated endotoxin-induced cardiac dysfunction and mortality in mice through a PI3K/Akt-dependent mechanism. *Shock* 2009;**32**:108–117.
19. Li J, Zhang Y, Li C, Xie J, Liu Y, Zhu W, Zhang X, Jiang S, Liu L, Ding Z. HSPA12B attenuates cardiac dysfunction and remodelling after myocardial infarction through an eNOS-dependent mechanism. *Cardiovasc Res* 2013;**99**:674–684.
20. Kong Q, Dai L, Wang Y, Zhang X, Li C, Jiang S, Li Y, Ding Z, Liu L. HSPA12B attenuated acute myocardial ischemia/reperfusion injury via maintaining endothelial integrity in a PI3K/Akt/mTOR-dependent mechanism. *Sci Rep* 2016;**6**:33636.
21. Liu L, Zhang X, Qian B, Min X, Gao X, Li C, Cheng Y, Huang J. Over-expression of heat shock protein 27 attenuates doxorubicin-induced cardiac dysfunction in mice. *Eur J Heart Fail* 2007;**9**:762–769.
22. Fan D, Takawale A, Shen M, Wang W, Wang X, Basu R, Oudit GY, Kassiri Z. Cardiomyocyte A disintegrin and metalloproteinase 17 (ADAM17) is essential in post-myocardial infarction repair by regulating angiogenesis. *Circ Heart Fail* 2015;**8**:970–979.
23. Gonzalez-Quesada C, Cavalera M, Biernacka A, Kong P, Lee DW, Saxena A, Frunza O, Dobaczewski M, Shinde A, Frangogiannis NG. Thrombospondin-1 induction in the diabetic myocardium stabilizes the cardiac matrix in addition to promoting vascular rarefaction through angiopoietin-2 upregulation. *Circ Res* 2013;**113**:1331–1344.
24. Fang L, Gao XM, Moore XL, Kiriazis H, Su Y, Ming Z, Lim YL, Dart AM, Du XJ. Differences in inflammation, MMP activation and collagen damage account for gender difference in murine cardiac rupture following myocardial infarction. *J Mol Cell Cardiol* 2007;**43**:535–544.
25. O'Neill LA. Targeting signal transduction as a strategy to treat inflammatory diseases. *Nat Rev Drug Discov* 2006;**5**:549–563.
26. Frantz S, Kobzik L, Kim YD, Fukazawa R, Medzhitov R, Lee RT, Kelly RA. Toll4 (TLR4) expression in cardiac myocytes in normal and failing myocardium. *J Clin Invest* 1999;**104**:271–280.

27. Satriano J, Schlondorff D. Activation and attenuation of transcription factor NF-kB in mouse glomerular mesangial cells in response to tumor necrosis factor-alpha, immunoglobulin G, and adenosine 3':5'-cyclic monophosphate. Evidence for involvement of reactive oxygen species. *J Clin Invest* 1994;**94**:1629–1636.
28. Sane DC, Mozingo WS, Becker RC. Cardiac rupture after myocardial infarction: new insights from murine models. *Cardiol Rev* 2009;**17**:293–299.
29. Schuster EH, Bulkley BH. Expansion of transmural myocardial infarction: a pathophysiologic factor in cardiac rupture. *Circulation* 1979;**60**:1532–1538.
30. Heymans S, Hirsch E, Anker SD, Aukrust P, Balligand JL, Cohen-Tervaert JW, Drexler H, Filippatos G, Felix SB, Gullestad L, Hilfiker-Kleiner D, Janssens S, Latini R, Neubauer G, Paulus WJ, Pieske B, Ponikowski P, Schroen B, Schultheiss HP, Tschope C, Van Bilsen M, Zannad F, McMurray J, Shah AM. Inflammation as a therapeutic target in heart failure? A scientific statement from the Translational Research Committee of the Heart Failure Association of the European Society of Cardiology. *Eur J Heart Fail* 2009;**11**:119–129.
31. Ma Y, Halade GV, Zhang J, Ramirez TA, Levin D, Voorhees A, Jin YF, Han HC, Manicone AM, Lindsey ML. Matrix metalloproteinase-28 deletion exacerbates cardiac dysfunction and rupture after myocardial infarction in mice by inhibiting M2 macrophage activation. *Circ Res* 2013;**112**:675–688.
32. Kempf T, Zarbock A, Widera C, Butz S, Stadtmann A, Rossaint J, Bolomini-Vittori M, Korf-Klingebiel M, Napp LC, Hansen B, Kanwischer A, Bavendiek U, Beutel G, Hapke M, Sauer MG, Laudanna C, Hogg N, Vestweber D, Wollert KC. GDF-15 is an inhibitor of leukocyte integrin activation required for survival after myocardial infarction in mice. *Nat Med* 2011;**17**:581–588.
33. Mezzaroma E, Toldo S, Farkas D, Seropian IM, Van Tassell BW, Salloum FN, Kannan HR, Menna AC, Voelkel NF, Abbate A. The inflammasome promotes adverse cardiac remodeling following acute myocardial infarction in the mouse. *Proc Natl Acad Sci USA* 2011;**108**:19725–19730.
34. Takahashi M. NLRP3 inflammasome as a novel player in myocardial infarction. *Int Heart J* 2014;**55**:101–105.
35. Takahashi M. Role of the inflammasome in myocardial infarction. *Trends Cardiovasc Med* 2011;**21**:37–41.
36. Mezzaroma E, Marchetti C, Toldo S. Letter by Mezzaroma, et al regarding article, "NLRP3 inflammasome as a therapeutic target in myocardial infarction". *Int Heart J* 2014;**55**:379.
37. Zeng Q, Jin C, Ao L, Cleveland JC Jr, Song R, Xu D, Fullerton DA, Meng X. Cross-talk between the Toll-like receptor 4 and Notch1 pathways augments the inflammatory response in the interstitial cells of stenotic human aortic valves. *Circulation* 2012;**126**:S222–S230.
38. Hamid T, Guo SZ, Kingery JR, Xiang X, Dawn B, Prabhu SD. Cardiomyocyte NF-kappaB p65 promotes adverse remodelling, apoptosis, and endoplasmic reticulum stress in heart failure. *Cardiovasc Res* 2011;**89**:129–138.
39. Frangogiannis NG. The inflammatory response in myocardial injury, repair, and remodelling. *Nat Rev Cardiol* 2014;**11**:255–265.